Review

The Extended Synaptotagmins of *Physcomitrium patens*

Alexander Kaier and Maria Ntefidou *

Posted Date: 3 March 2025

doi: 10.20944/preprints202503.0048.v1

Keywords: extended synaptotagmins; membrane contact sites; lipid transport proteins; tip growth; plasmodesmata; *Physcomitrium patens*; bryophytes

 doi:10.20944/preprints202503.0048.v1

Review

The Extended Synaptotagmins of *Physcomitrium patens*

Alexander Kaier [1] and Maria Ntefidou [2,*]

[1] Division of Biochemistry, Department of Biology, Friedrich-Alexander-University Erlangen-Nuremberg, 91058 Erlangen, Germany

[2] Division of Cell Biology, Department of Biology, Friedrich-Alexander-University Erlangen-Nuremberg, 91058 Erlangen, Germany

* Correspondence: maria.ntefidou@fau.de

Abstract: Membrane contact sites (MCSs) between the endoplasmic reticulum and the plasma membrane enable transport of lipids without membrane fusion in eukaryotes. Extended Synaptotagmins (ESYTs) can form and maintain MCSs, acting as tethers between two membrane compartments. In plants, ESYTs have been mainly investigated in the flowering plant Arabidopsis and shown to maintain the integrity of the plasma membrane, especially during stress responses such as cold acclimatization, mechanical trauma and salt stress. ESYTs are also present at MCSs of plasmodesmata, where they regulate defense responses by modulating cell-to-cell transfer of pathogens. Here, the analyis of ESYTs in plants was expanded to the bryophyte *Physcomitrium patens*, an extant representative of the earliest land plant lineages. *P. patens* was found to contain a larger number of ESYTs that were distributed in all previously established classes and an additional class not present in Arabidospsis. Motif discovery identified regions in the Synaptotagmin-like mitochondrial (SMP) domain that may explain phylogenetic relationships as well as protein function. These findings highlight the suitability of *P. patens* as a model organsim to study ESYT functions in tip growth, stress-responses and plasmodesmata-mediated transport, and open new directions of research regarding the function of MCSs in cellular processes and plant evolution.

Keywords: extended synaptotagmins; membrane contact sites; lipid transport proteins; tip growth; plasmodesmata; *Physcomitrium patens*; bryophytes

1. Introduction

Extended Synaptotagmins (ESYTs) are integral membrane proteins of the endoplasmic reticulum (ER) that play an essential role in establishing and maintaining membrane contact sites (MCS) [1–3]. These specialized regions are sites of close appositions of membranes between the ER and the plasma membrane (PM) or another organelle. ESYTs are conserved across eukaryotes and, due to their tethering function in MCSs, contribute to lipid transfer and calcium homeostasis [4]. In plants, ESYTs have been studied primarily in angiosperms, where they support adaptation to environmental stresses by maintaining the integrity of the PM and regulating signaling pathways [5,6]. Notably, plant ESYT homologues have been implicated in MCSs at plasmodesmata, the intercellular channels that connect neighboring plant cells and are crucial for communication, cell-to-cell transport of metabolites, signals and even pathogens and are essential for coordinated tissue development in plants with complex body plans. At plasmodesmata, ESYT homologues participate in immune responses, underscoring the multiple functions of ESYTs in angiosperms.

This review explores the ESYTs of *Physcomitrium patens*, a model bryophyte representing one of the earliest lineages of land plants. The ESYT family of *P. patens* is compared with those of two other bryophytes *Sphagnum fallax* and *Marchantia polymorpha* as well as to the angiosperm *Arabidopsis thaliana* and the well-studied ESYT homologues of *Homo sapiens* and *Saccharomyces cerevisiae*. *P. patens*

 doi:10.20944/preprints202503.0048.v1

is an ideal system to examine the roles of ESYTs in the membrane dynamics taking place at MCSs and in plasmodesmata-mediated intercellular processes. Additionally, the evolutionary position of *P. patens* can offer insights into the functional diversification of ESYTs and their significance in the early adaptation of land plants to their habitat.

2. ESYTs in Plants

2.1. Membrane Contact Sites

The transport of lipids, proteins and other cargo is primarily facilitated by vesicle trafficking, which supports cellular growth and maintenance [7,8]. However, cells also employ an alternative mechanism that allows direct exchange of metabolites and signaling molecules at MCSs between membrane compartments [9]. MCSs were first observed at the interface between the ER and the PM [10], and subsequent studies revealed that the ER interacts with all major organelles, including mitochondria, chloroplasts, lysosomes and the Golgi apparatus [11–15] to enable direct communication, lipid exchange, and regulation of ion dynamics in signaling pathways [9]. MCSs are characterized by the close apposition between two membranes, without resulting in membrane fusion [16]. These sites are tethered by proteins that physically connect the two membrane compartments and can be either static or dynamic with rapid turnover [17,18] (Figure 1). ESYTs belong to an expanding group of proteins that function as tethers at MCSs in plants, animals and yeast, where they are known as Tricalbins (TCBs) [3,5,19,20]. Other MCSs tethers include Vesicle-Associated membrane Protein-associated proteins (VAPs) [21,22] and oxysterol-binding proteins (ORPs) [23,24]. In addition, tethers can connect MCSs to the cytoskeleton. For example, the plant-specific actin-binding NET3C protein, which belongs to the NETWORK protein family, forms dimers that connect the ER and PM at the C-termini and also bind to actin filaments, thereby linking the MCSs to the cytoskeleton [21]. NET3Cs can also interact with VAP27s [25] or kinesin-light-chain-related protein 1 [26], which are associated with microtubules further expanding the physical and functional connection between MCSs and the cytoskeleton. Beyond mechanically connecting membranes, MCSs contribute to organelle dynamics, as has been observed in mitochondrial fission in yeast and mammalian cells [27,28] and in the autophagy of mitochondria in plants [29], topics that will not be further addressed in this review.

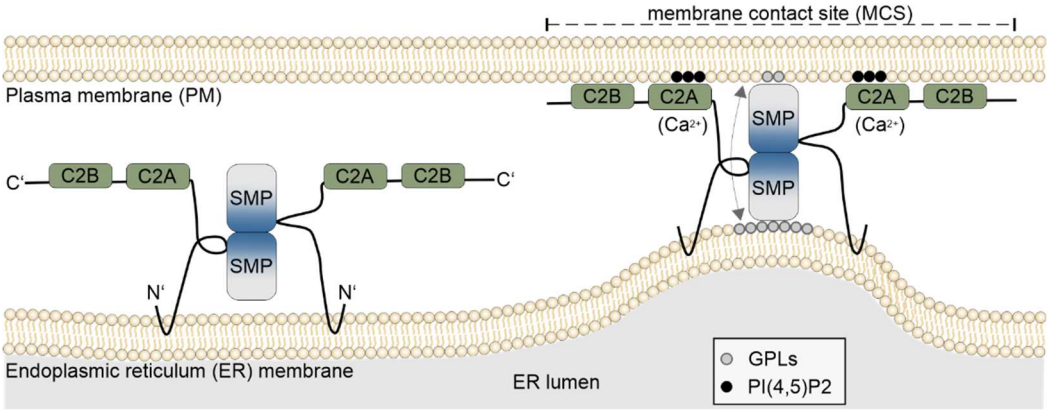

Figure 1. Schematic drawing of Extended Synaptotagmins. ESYT dimers are anchored by their N-terminus to the endoplasmic reticulum (ER) while Ca^{2+}-dependent membrane-targeting domains (C2: green box) at the C-terminus can bind to the plasma membrane (PM), depending on the presence of Ca^{2+} ions and the local lipid composition of the PM [50]. Attachment of ESYTs to the PM forms tethers that reduce the distance between the two membrane compartments, creating a membrane contact site (MCS). The two Synaptotagmin-like Mitochondrial-lipid-binding Protein (SMP: grey-blue gradient box) domains form a dimer by interacting in an antiparallel configuration at their respective C-terminal end and associating at their N-terminal regions with the ER and the PM, allowing the transfer of lipids between the ER and the PM, causing changes in the lipid composition at the MCS. One such example is the transfer of glycerophospholipids (GPLs) e. g.

 doi:10.20944/preprints202503.0048.v1

phosphatidylethanolamine, phosphatidylcholine and phosphatidylserine from the ER to the PM, but ESYTs can exchange lipids in both directions.

A well-documented function of MCSs in yeast, animals and plants is the exchange of lipids between the ER and PM or between the ER and other organelles [9]. For instance, during cold stress, the ESYT homologues AtSYT1 and AtSYT3 in *Arabidopsis thaliana* regulate the transport of diacylglycerol (DAG) at ER–PM MCSs, ensuring the maintenance of DAG homeostasis at the PM [30]. Compared to vesicle exocytosis, lipid transfer via MCSs has been proposed to offer the advantage of enabling rapid and localized changes in the lipid composition of the PM due to the short distance between the two membrane compartments [31]. In animals MCSs regulate calcium homeostasis. Human ESYTs (HsESYTs) organize the clustering of the Stromal Interaction Molecule-1 (STIM) [32], a calcium sensor embedded in the ER, that oligomerizes and relocates to MCSs upon Ca^{2+} depletion. This relocation leads to the activation of PM-localized Calcium Release-Activated Calcium Modulator 1 (CRACM1, ORAI1) [33–35] resulting in Ca^{2+} influx known as store-operated Ca^{2+} entry (SOCE) [17,36].

2.2. Domain Structure and Functions of ESYTs

ESYTs are found in all eukaryotes and are structurally characterized by three features: a) an N-terminal hydrophobic region, b) a single Synaptotagmin-like Mitochondrial-lipid-binding Protein (SMP) domain, and c) a variable number of C2, Ca^{2+}-dependent membrane-targeting domains first identified in protein kinase C [37] (Figure 1). Based on the presence of C2 domains, ESYTs were named after the Synaptotagmins (SYTs), a protein family predominantly expressed in the nervous system of animals and characterized by two C2 domains [38]. In neurons, SYTs regulate the fusion of synaptic vesicles to the PM during calcium-regulated exocytosis of neurotransmitters, playing a critical role in synaptic transmission [39–43]. SYTs are specific to animals and are absent in yeast, plants and other organisms.

Unlike SYTs, ESYTs are stably anchored to the outer leaflet of the ER membrane by two N-terminal hydrophobic regions that form a hairpin structure. This configuration leaves the N-terminus and the remaining protein sequence exposed in the cytoplasm (Figure 1), distinguishing them from SYTs, which are bound to vesicles. Structural analysis of HsESYTs revealed the presence of an SMP domain, absent in SYTs, that adopts a cylindrical structure with a hydrophobic core [44,45]. This places ESYTs within the Tubular lipid-binding (TULIP) domain family, which includes prokaryotic and eukaryotic proteins involved in lipid sensing and transport [4,46,47]. Although SMP domains are not required for tethering ESYTs to the PM [3,44,48,49], they can transiently associate with membranes at their N-terminal tip and sense membrane curvature, exhibiting a preference for curved regions of bilayers found in the tubules of the cortical ER [50]. Indeed, ESYT homologues that localize at ER–PM MCSs such as AtSYT1 and HsESYT1, preferentially accumulate and are anchored at tubular ER in the cell cortex, placing them in the vicinity of the PM [50,51]. The function of the SMP domains of HsESYTs, ScTCBs [2,46,52] and the Arabidopsis homologues (AtSYTs) [53] is to bind and exchange lipids between the ER and the PM [20,50]. While the mechanism of lipid transfer by SMP domains is not fully understood, a model for HsESYTs describes SMP domains of two HsESYTs forming a homo- or heterodimer in an antiparallel configuration trough interaction at their respective C-terminal end. These dimers then associate with their N-terminal tips at the ER and the PM, respectively (Figure 1) [46]. The SMP domains contain a hydrophobic groove that can bind glycerophospholipids at one membrane, followed by a flipping motion along the vertical axis of the dimer to release the lipids at the other membrane compartment [50]. Whether this mechanism applies to other ESYT homologues remains to be investigated. Structural analysis of AtSYT1 supports a similar dimerization mechanism based on SMP domain interaction at their C-terminal termini [53]. Notably, the lipid selectivity of SMP domains is low, instead a broad spectrum of anionic glycerophospholipids were shown to be transferred by HsESYTs, ScTCBs and AtSYTs [20,46,50,53,54].

 doi:10.20944/preprints202503.0048.v1

At the C-terminal end, tandem-arranged C2 domains mediate interaction with the PM, bridging the ER and PM with an average inter-membrane distance of approximately 10–30 nm [55,56]. This tethering is reversible and does not result in membrane fusion, a key feature distinguishing MCSs from the vesicle fusion processes regulated by SYTs in neuronal cells during exocytosis. Some C2 domains in ESYTs exhibit Ca^{2+}-dependent binding to specific acidic phospholipids [57], such as phosphatidylinositol 4,5-bisphophate (PI [4,5]P2) at the PM, while others lack calcium-binding capability [58]. The number of Ca^{2+} ions bound by ESYT C2 domains varies from 2–4 [58], similar to the variability observed in some of the C2 domains of SYTs while other C2 domains possess mutations preventing the binding of Ca^{2+} ions [59]. This variability suggests a complex regulatory mechanism for C2 domain interactions with the PM, possibly involving additional roles beyond Ca^{2+}-dependent tethering [3,57].

2.3. ESYTs in Arabidopsis

The initial plant ESYT homologues were identified in *Arabidopsis thaliana* and were designated as SYTs [5,60] before the comprehensive characterization of the ESYTs in animals. In this review, we follow the established nomenclature for Arabidopsis homologues (AtSYTs and AtNTMC2T6s). Newly identified members in bryophytes, however, will be referred to as ESYTs until further structural and functional data are available for their classification. Plant ESYT homologues share a similar domain structure with their animal and yeast counterparts, with three notable differences: a) the N-terminal hydrophobic region does not consistently form a hairpin, instead some ESYT homologues possess a single transmembrane region, resulting in the N-terminal end not being exposed to the cytoplasm, b) typically contain only 1–3 C2 domains, compared to the 3–5 in animal or yeast homologues, and c) the role of Ca^{2+} in regulating of C2 domain binding to the PM may differ. Targeting of AtSYT1 to the PM requires both of its C2 domains as demonstrated by truncation analysis, which showed that PM localization occurs only when both C2 domains are present [56]. This is consistent with the mechanism observed in HsESYTs and ScTCBs where multiple C2 domains mediate PM attachment [61]. This raises the question of how plant ESYTs with a single C2 domain target the PM. In HsSYT1, which contains two C2 domains, the second C2 domain (C2B) is sufficient for Ca^{2+}-dependent binding to phospholipids [62,63]. Another mechanism of PM targeting is seen in HsTMEM24, an SMP domain containing protein with a single C2 domain that is anchored to the ER. Although HsTMEM24 exhibits low sequence homology to ESYTs, it localizes at MCSs regulating signaling functions in neurons and insulin secretion in pancreatic cells based on a mechanism of Ca^{2+}-dependent lipid transport from the ER to the PM [64–66]. HsTMEM24 associates with the PM through its polybasic C-terminal region, which interacts with anionic lipids. The binding to the PM is supported but does not dependent on the C2 domain. Notably, HsTMEM24 binds to the PM at low cytosolic Ca^{2+}, whereas an increase in Ca^{2+} activates protein kinase C, which in turn phosphorylates residues at the C-terminal polybasic region, thereby inhibiting PM association [67]. It remains to be determined whether plant ESYTs with a single C2 domain rely on similar mechanisms.

In Arabidopsis, seven ESYT homologues (AtSYT1–AtSYT7) have been grouped into four classes through phylogenetic analysis [19], and two AtNTMC2T6s forming an additional class closely related to AtSYT6 [68]. AtSYTs possess a domain structure similar to animal and yeast homologues consisting of i) an N-terminal hydrophobic region either consisting of a single transmembrane domain or forming a hairpin structure, ii) an SMP domain and iii) 1–3 C2 domains arranged in tandem at the C-terminus (Table S1) [5,19,68–70]. Other proteins containing an SMP and C2 domains, but with additional domains or hydrophobic regions located at the C-terminus, are not included in this review. AtSYTs of Arabidopsis dimerize, attach to the PM through binding of the C2 domains to phosphoinositides or phosphatidylserine [18,53,71], generate MCSs and transfer lipids between the ER and the PM similarly to animal and yeast counterparts [3,52]. However, some AtSYTs localize at MCSs between the ER and the trans-Golgi-network (TGN) suggesting additional functions of plant ESYTs [68].

 doi:10.20944/preprints202503.0048.v1

AtSYT1 and AtSYT5 are expressed in all tissues, with AtSYT1 displaying the highest expression of all AtSYTs [72], while other homologues show tissue-specific expression as seen in the expression of AtSYT4 in the phloem [73]. The cellular localization of AtSYTs has been examined using approaches such as fluorescent protein tagging under the endogenous promoter in *A. thaliana*, transient heterologous expression in *Nicotiana benthamiana* leaves, and immunolabeling. The intracellular localization of AtSYT1–AtSYT3, AtSYT5 and AtSYT7 (also known as AtCLB1 or AtNTMC2T4) resembles the localization of HsESYTs and ScTCBs, by displaying a punctate appearance at the cortical region of cells, and colocalizing with markers of the ER, PM and MCSs, confirming their roles in MCSs of the ER-PM interface [5,18,30,69,74]. Although an AtSYT2-GFP fusion protein was initially reported to localize at the TGN [75], later studies using immunofluorescence labeling of anti-AtSYT2 in pollen tubes revealed that AtSYT2 localizes both to the TGN and the PM [74]. AtSYT2 localization at the PM was also supported by AtSYT2-DsRED-E5 and was shown to be delivered to the PM from the TGN through conventional secretion [74]. AtSYT4 is primarily expressed in sieve elements precursors and localizes in the cytoplasm concentrating around the nucleus or at the cell cortex depending on the developmental stage of the phloem [73]. AtSYT6 and AtNTMC2T6s have been shown to localize at the ER and colocalize with the TGN marker Vesicle-Associated Membrane Protein 721 (VAMP721) [76], suggesting roles in forming of ER-TGN membrane contact sites [68,77].

AtSYT1 not only generates and maintains ER–PM MCSs in Arabidopsis leaf cells but also contributes to a second type of MCSs as a complex with VAP27 [78]. Deletion of AtSYTs has revealed roles in stress responses related to mechanical, cold and ionic stresses, implicating functions in plasma membrane dynamics and repair mechanisms. AtSYT1 provides tolerance to freeze-induced puncture wounds, with extracellular calcium enhancing this effect, indicating a role in calcium-dependent PM resealing [60]. AtSYT1 expression was upregulated in response to mechanical stress, again suggesting a protective role in PM stability [18].

AtSYTs participate in multiple processes by assembling into homo- and heterodimers and forming complexes with other ESYTs [30,53], similar to HsESYTs and ScTCBs [50,79]. For example, seedlings grown under salt stress were more affected in At*syt1* At*syt2* double compared to single knockouts, due to increased PM permeability [5]. Fluorescent labeling of MCSs has shown that salt-stress induces the relocation of AtSYT1 to the cortical ER. This process is dependent on an increase in PI(4,5)P2 at the PM and leads to an expansion of the area occupied by MCSs. Interestingly, while the cortical cytoskeleton was not required to maintain MCSs, it was essential for AtSYT1 accumulation at these sites [71]. Additionally, stress induced by trivalent lanthanum and gadolinium increased phosphatidylinositol-4-phosphate (PI4P) levels at the PM, resulting in the accumulation of a complex composed of AtSYT1, AtSYT5 and AtSYT7 at ER–PM MCSs [69]. These findings further support the idea that AtSYT relocation is driven by increases in PI4P or PI(4,5)P2 at the PM in response to stress. While AtSYT1, AtSYT5 and AtSYT7 do not directly interact with the mechanosensitive ion channel AtMSL10 as in the case of VAP27, they are functionally related to AtMSL10 [80], a key sensor and regulator of osmotic, salt and mechanical stress [81]. Under cold stress, AtSYT1 and AtSYT3 bind PI4P at the PM, leading to MCSs rearrangement and removal of excess DAG. These AtSYTs showed no selectivity for specific DAG species, and the removal of DAG from the PM was identified as a general mechanism for maintaining lipid homeostasis at the PM in response to abiotic stress [30].

AtSYT1 and AtSYT2 have also been reported to influence pollen germination and pollen tip growth, however, gene knockouts resulted in only mild growth defects [74]. Unlike the essential role of Ca^{2+} in regulating the association of some of the C2 domains to PI(4,5)P2 at the PM [54,57] in animal and yeast ESYT homologues, and HsESYTs functioning as calcium sensors and controlling the Ca^{2+}-content of the ER through the SOCE mechanism [82], the role of calcium in plant ESYT homologues appears to be different. The C2A domain of AtSYT1 binds Ca^{2+}, which enhances its interaction to phosphatidylserine but is not required for binding PI(4,5)P2 or other types of phosphoinositides at the PM [18,83]. The C2B protein sequence of AtSYT1 does not contain a Ca^{2+}-binding signature and

 doi:10.20944/preprints202503.0048.v1

was proven experimentally to bind phosphoinositides and phosphatidylserine independent of Ca^{2+} [18,53] implying a different contribution of Ca^{2+} to the interaction of AtSYT1 with the PM compared to ESYT homologues of animals and yeast.

Several AtSYTs localize to MCSs of plasmodesmata with positive or negative effects on immune responses, as reviewed in detail by Benitez-Fuente et al. [6]. Plasmodesmata connect plant cells across their cell walls, forming the symplast [84], and are essential for transporting nutrients, nucleic acids and signaling in plant tissues, all processes that were fundamental for the development of land plants with complex body plans [85]. Pathogens exploit plasmodesmata to spread from cell-to-cell during infection, using a variety of mechanisms, with some viruses using movement proteins to modify the permeability of the plasmodesmata. The structure of a plasmodesma consists of a cytoplasmic sleeve that is surrounded by the PM and traversed by a narrow ER tubule, the desmotubule [86]. The PM is connected to the desmotubule by protein tethers, including AtSYTs [19,87], and the MCSs they form are important in defense responses. AtSYT1 was shown to physically interact with AtSYT5 and AtSYT7 and to colocalize at MCSs. Triple knock-out of At*syt1* At*syt5* At*syt7* caused defects in the morphology of ER tubules and increased the diameter of the ER at the entrance to plasmodesmata, indicating that AtSYT1, AtSYT5 and AtSYT7 have a role in constricting the ER, which is required for desmotubule formation [88]. The triple knock-out inhibited cell-to-cell transfer of a movement protein related to the *Tobacco mosaic virus* but not free GFP and suppressed infection rates, indicating that AtSYT1, ATSYT5 and AtSYT7 are used by the virus for their active transport through plasmodesmata [19]. In other cases, AtSYTs have beneficial effects on the immune response, as in the case of AtSYT1, AtSYT4 and AtSYT5, which confer resistance to the bacterial pathogen *P. syringae* [89].

2.4. P. patens as a Model Organism for Membrane Dynamics

Physcomitrium patens is a moss bryophyte that is characterized by a dominant haploid gametophyte stage and a short-lived diploid sporophyte stage [90]. Its life cycle begins with haploid spores, that germinate into branched, filamentous protonemata. The apical initial (stem) cells have a dual role in cell proliferation and cell growth. Cell expansion in these apical cells occurs by tip growth [91], a highly polarized form of cell expansion where the growth zone is confined to the apical region of the PM, resulting in elongated cells (Figure 2). Protonemata consist of two cell types that develop sequentially: chloronemata, which primarily function in photosynthesis, and caulonemata, which facilitate the expansion of the colony into suitable habitats and the uptake of nutrients. The first cells, chloronemata, emerge directly from spores (or protoplasts), contain large chloroplasts and are separated from neighboring cells by cell walls oriented perpendicular to the growth axis. Depending on auxin signaling and environmental cues, chloronemata can differentiate into caulonemata [92,93]. Compared to chloronemata, caulonemata exhibit faster rates of tip growth and cell division, possess fewer and smaller chloroplasts, and neighboring cells are separated by obliquely oriented cell walls [92,94,95]. For their growth, caulonemata rely on energy obtained from the photosynthesis of chloronemata or from external sources, such as glucose [94,96,97]. On both chloronemata and caulonemata, side branch initial cells arise, which generate new filaments on chloronemata, while on caulonemata, they either develop new filaments or produce a bud by undergoing a series of programmed longitudinally and transverse cell divisions, depending on hormonal regulation by cytokinin and environmental factors such as light quality [98,99]. Buds develop into gametophores [100], a shoot-like structure (Figure 2) with leaf-like phyllids and rhizoids, which are chloroplast-free filaments at the base of the gametophore. Rhizoids resemble caulonemata, with apical initial cells that expand by tip growth, and function in anchoring the gametophore to the substrate and the uptake of water and nutrients [101]. At the apex of the gametophore, male and female gametangia develop (monoicous plant) that, upon fertilization, produce the diploid sporophyte. The sporophyte undergoes meiosis to produce haploid spores, thereby completing the life cycle.

 doi:10.20944/preprints202503.0048.v1

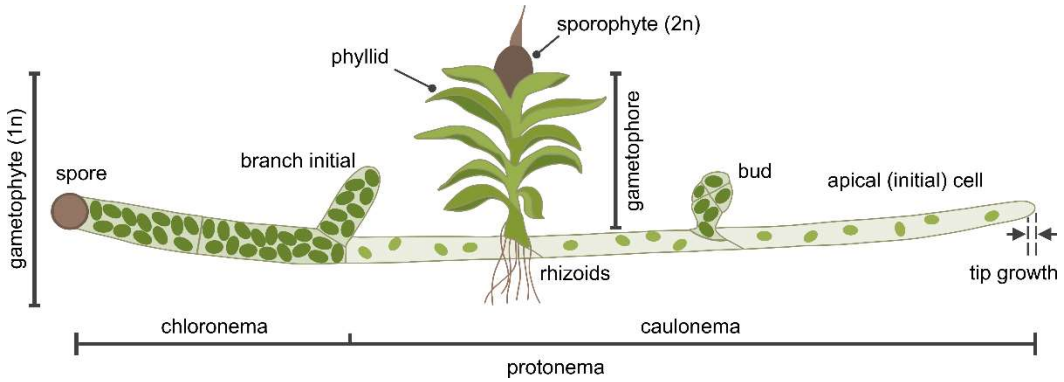

Figure 2. Schematic depiction of *P. patens* development. The haploid gametophyte stage begins with a spore, which, after its first cell division, gives rise to chloronema cells containing numerous large chloroplasts and perpendicular cell walls between neighboring cells. Chloronemata differentiate into caulonemata, which have fewer, smaller chloroplasts and are separated by oblique cell walls. Together, chloronema and caulonema cells form the protonema tissue. The apical (initial) cell of each filament expands through tip growth and is the only cell that divides. Side branch initial cells form new filaments. These cells may develop into filaments identical to the main filament or into buds that grow into gametophores, composed of leaf-like structures (phyllids) and rhizoids. At the center of the gametophore apical region, male and female reproductive tissues develop (not shown), leading to the formation of the diploid sporophyte upon fertilization. After maturation, the sporophyte releases haploid spores, completing the life cycle of *P. patens*. Not to scale.

The simple structure of *P. patens*, its extensive haploid tissues, an excellent annotated genome database [102], and availability of a broad methodology for molecular biology, biochemistry and microscopic analysis have established *P. patens* as a model plant organism in many areas of research [90]. *P. patens* is especially suited for the study of membrane dynamics due to its evolutionary position as an extant representative of the first plants to transition from water to land, possessing features that demonstrate the evolution of adaptations during plant terrestrialization.

While plasmodesmata are found in some algae, they exhibit a simple structure without a desmotubule [103]. In bryophytes, plasmodesmata are fully developed and are considered to have been essential in the emergence of land plants [104]. Indeed, the plasmodesmata of *P. patens* share many features found in vascular plants, including angiosperms [104,105], thus providing an ideal system for investigating the role of ESYTs in plasmodesmata. The protonema offers an additional advantage for the investigation of plasmodesmata due to the linear arrangement of chloroplast-rich chloronemata followed by chloroplast-poor caulonemata. Both cell types can be viewed as the two parts of a source-sink model, since caulonemata are believed to rely on the photoassimilates supplied by chloronemata to fulfill their energy requirements [106]. This is further supported by the lack of long-term-survival in caulonema-only mutants, whereas viable mutants consisting exclusively of chloronemata have been reported [92,94].

Knowledge of ESYTs in plants is limited to the angiosperm *A. thaliana*. In this review, the putative ESYTs of the bryophytes *Physcomitrium patens*, *Sphagnum fallax* and *Marchantia polymorpha* will be reported and compared to *Arabidopsis thaliana* in order to provide insight into the ESYT family at an early stage of plant evolution.

2.5. ESYTs in Bryophytes

Using the amino acid sequence of either full-length proteins or SMP domains of AtSYTs, AtNTMC2T6 or HsESYT1, the genome databases of *P. patens*, *S. fallax* and *M. polymorpha* were searched. The identified ESYTs were then used as baits to re-scan the bryophyte genomes in order to find sequences not detected using heterologous ESYTs. 15 *ESYT* genes were identified in *P. patens* (Pp*ESYT1-15*), 15 *ESYT* homologues were found in *S. fallax* (Sf*ESYT1-15*) and 10 *ESYT* homologues in *M. polymorpha* (Mp*ESYT1-10*, Table 1). Only sequences containing the typical configuration of ESYTs composed of i) 1–2 N-terminal hydrophobic region(s), ii) an SMP domain, iii) at least one C2

 doi:10.20944/preprints202503.0048.v1

domain, and iv) no other domains or additional hydrophobic regions at the C-terminus, were included for further analysis. PpESYT1–3 [70] and PpESYT1–8 were reported previously [19]. An additional PpESYT (XP_024382745) was identified previously using the sequence database of the National Center for Biotechnology Information (NCBI) [19]. This ESYT differs from PpESYT15, as identified in this work using the latest annotation of the *P. patens* genome [102], by containing a 17 amino acids deletion in the SMP domain and a 12 amino acids insertion in the C2 domain.

Multiple sequence alignment (MSA) of the 56 amino acid sequences showed that the sequence lengths vary strongly, with MpESYT7 on one end of the spectrum consisting of 447 residues and ScTCB3 on the other end with 1545 residues (Table S1). The alignment and the consensus sequence show strong divergence between the sequences, even within conserved regions (Figure S1). However, for some positions in the alignment, strong consensus was detected. At alignment positions 278 and 291, both of which are located in the SMP domain, all analyzed sequences except HsTMEM24 contained tryptophan (W). All sequences shared Asparagine (N) at alignment position 280. These positions, among others, indicate strong conservation and imply functional importance of these residues in the SMPs across all tested phylogenetic groups. The weak sequence homology of HsTMEM24 to all other sequences was expected and is in accordance with its classification outside the HsESYT gene family. Despite this, HsTMEM24 was included in this study because it i) possesses the domain structure of ESYTs but with a single C2 domain, ii) forms MCSs between the ER and the PM and iii) transfers lipids between the two membrane compartments [65,66]. Some of the putative ESYTs in bryophytes which were identified in this study possessed a single C2 domain and were clustered together with known ESYTs including HsESYTs and ScTCBs, all of which contain at least three C2 domains. This finding, along with the phylogenetic isolation of HsTMEM24 from all other sequences, may indicate that plant-based ESYTs with a single C2 indeed belong to the ESYT gene family (Figure 3).

The protein sequences of ESYT homologues that we identified in bryophytes were also compared to those of *A. thaliana*, the only ESYT-like family in plants analyzed in detail so far. AtSYTs cluster in 4 classes [19] while AtNTMC2T6s form a fifth class with a protein structure, cellular localization and sequence homology related to AtSYT6 [68]. Previous phylogenetic analyses further revealed that class I (AtSYT1, AtSYT2, AtSYT3), class II (AtSYT4, AtSYT5) and class III (AtSYT7) form a clade with a different phylogenetic origin than class IV (AtSYT6) [19]. The ESYT homologues identified in bryophytes were distributed in all five classes and formed an additional class VI that did not contain any AtSYTs (Table 1, Figure 3, see Figure S2 for explicit branch lengths of the phylogenetic tree). In each class, the number of ESYT homologues in bryophytes varied slightly compared to *A. thaliana* but remarkably, the overall trend seems to be that the ancestors of the first terrestrial plants already possessed ESYT homologues for all classes as identified in Arabidopsis, with the exception of class VI. Interestingly, class VI contained putative bryophyte ESYT genes for which no homologue exists in Arabidopsis. These sequences possess two N-terminal hydrophobic regions, probably forming a hairpin structure, an SMP domain and one C2 domain (Table 1, Figure 3).

The bryophyte *Physcomitrium patens* is a basal land plant and an extant representative of the first plants to succeed in land colonization and form a sister clade to vascular plants. Due to its evolutionary position, *P. patens* is widely utilized to uncover the mechanisms for adaptation of plants on land [107,108]. In our analysis *P. patens* contained more ESYTs (15) than previously reported and also more than the angiosperm *A. thaliana* [19] (Table 1). The increased number of ESYTs in *P. patens* was consistent with an equal number of ESYT homologues identified in *S. fallax* (15). Interestingly, for *M. polymorpha*, a bryophyte from the clade of liverworts, 10 putative ESYT homologues were identified, comparable to the number of ESYTs in *A. thaliana* (9). In contrast to *P. patens* and *S. fallax*, *M. polymorpha* has not been subjected to whole genome duplications (WGDs), suggesting that the large ESYT families of *P. patens* and *S. fallax* are partially independent of WGDs. The identification of ESYTs in bryophytes is in agreement with the presence of ESYTs in *Klebsormidium nitens* [19], a terrestrial alga known to exhibit early signs of adaptation mechanisms observed in land plants [109]. The ESYTs of *K. nitens* have been postulated to have participated in the development and function of

 doi:10.20944/preprints202503.0048.v1

plasmodesmata, potentially contributing to the adaptation of basal plants to terrestrial conditions [19,109].

Table 1. ESYT-like homologues of *Arabidopsis thaliana, Physcomitrium patens, Sphagnum fallax* and *Marchantia polymorpha*. Distribution of the number of ESYT and AtNTMC2T6 homologues based on phylogenetic analysis (see Figure 3) in classes I to IV described by Ishikawa et al., [19] and class V reported by Huercano et al., [68]. Class VI did not contain AtSYTs.

	Class I	Class II	Class III	Class IV	Class V	Class VI	Total
A. thaliana	3	2	1	1	2	0	9
M. polymorpha	2	1	2	1	2	1	9[1]
S. fallax	4	0	1	3	5	2	15
P. patens	3	1	3	2	5	1	15

[1] MPESYT10 did not belong to classes I–VI.

The structure of the phylogenetic tree, which was constructed using the maximum likelihood method [110], was further supported by the heatmap containing pairwise distances between sequences (Figure S3). It is important to note that the distances were not used for the construction of the tree, but show another aspect of sequence similarity. The Figure shows that HsTMEM24 is indeed rather different from all other investigated genes. Also, the genes in class IV show very low sequence similarity to all other putative ESYTs that were analyzed in this study. The genes in class V show lower sequence similarity between each other than the sequences of other classes, like class I, class III and class IV, indicating a stronger evolutionary divergence than sequences within other classes. This observation is also reflected in the branch lengths of the phylogenetic tree.

SMP domains of ESYTs have essential roles at MCSs in i) forming homo- and hetero-dimers, ii) sensing the curvature of the membrane bilayer, thus contributing to the localization of ESYTs at the tubular ER of the cell cortex, and iii) binding and transferring lipids between membrane compartments [4,50,53]. Sequence comparison of the SMP domains of HsESYTs and ScTCBs showed sequence conservation in the C-terminal end of SMP domains corresponding to the region of SMP dimerization [46]. In addition to HsESYTs and ScTCBs, the alignment performed in this study included putative ESYT homologues of plants, revealing a few highly conserved residues located at the N-terminal end of the SMP domains, the region of the domain that associates with the PM or the ER (Figure S1). A further comparison of the SMP domains was carried out using the Multiple EM for Motif Elicitation tool (MEME) [111]. The MEME analysis revealed with a few exceptions the presence of two conserved motifs M1 and M7 at the N- and C-terminal region of the SMP domain, respectively (Figure 3). This indicates that the SMP regions needed for interaction with membrane bilayers or dimerization are conserved across the examined phylogenetic groups. The high conservation of the M1 motif at the region of the SMP domain that interacts with different membranes (e. g. the ER, PM, TGN) could imply a low specificity of the SMP binding to the lipid composition of membranes. This is in agreement with the finding that SMP domains are dispensable for the tethering of HsESYTs at MCSs but function as sensors of membrane curvature [50]. The conserved M7 domain located at the interface of SMP dimerization is consistent with the ability of ESYTs to form homo- and heterodimers in animals, yeast and plants, as well as the participation of the same ESYT in several complexes. This behavior is exemplified by AtSYT1, which together with AtSYT3, regulates PM integrity in cold stress responses [30], while interacting with AtSYT5 and ATSYT7 in immune responses [19]. Exceptions to the conservation of the M1 and M7 motifs include MpESYT3 which was missing the M1 motif, and AtSYT1, MpESYT10, ScTCB1, ScTCB2 which lacked the M7 motif at the C-terminus of the SMP domain. HsTMEM24 is the only sequence that does not contain any of the overrepresented motifs in the analyzed SMP domains, providing further evidence for its distinctiveness from the remaining sequences in terms of molecular structure. The core region of the SMP domain, which contains the hydrophobic groove for lipid binding, proves to be more variable than the terminal regions of the domain. The distribution of SMP motif composition throughout the phylogenetic tree aligns with the

 doi:10.20944/preprints202503.0048.v1

class formation to some degree. All sequences with SMP motif M6 are found in class I, which contains no other sequences. The same is true for the genes with SMP motif M3, that are part of class V. These observations strongly indicate that the genes within the respective classes, stemming from different species, form orthologues and may therefore share physiological function within the respective organism. Interestingly, almost all classes, with exception of class II and VI, contain genes from all analyzed plant species.

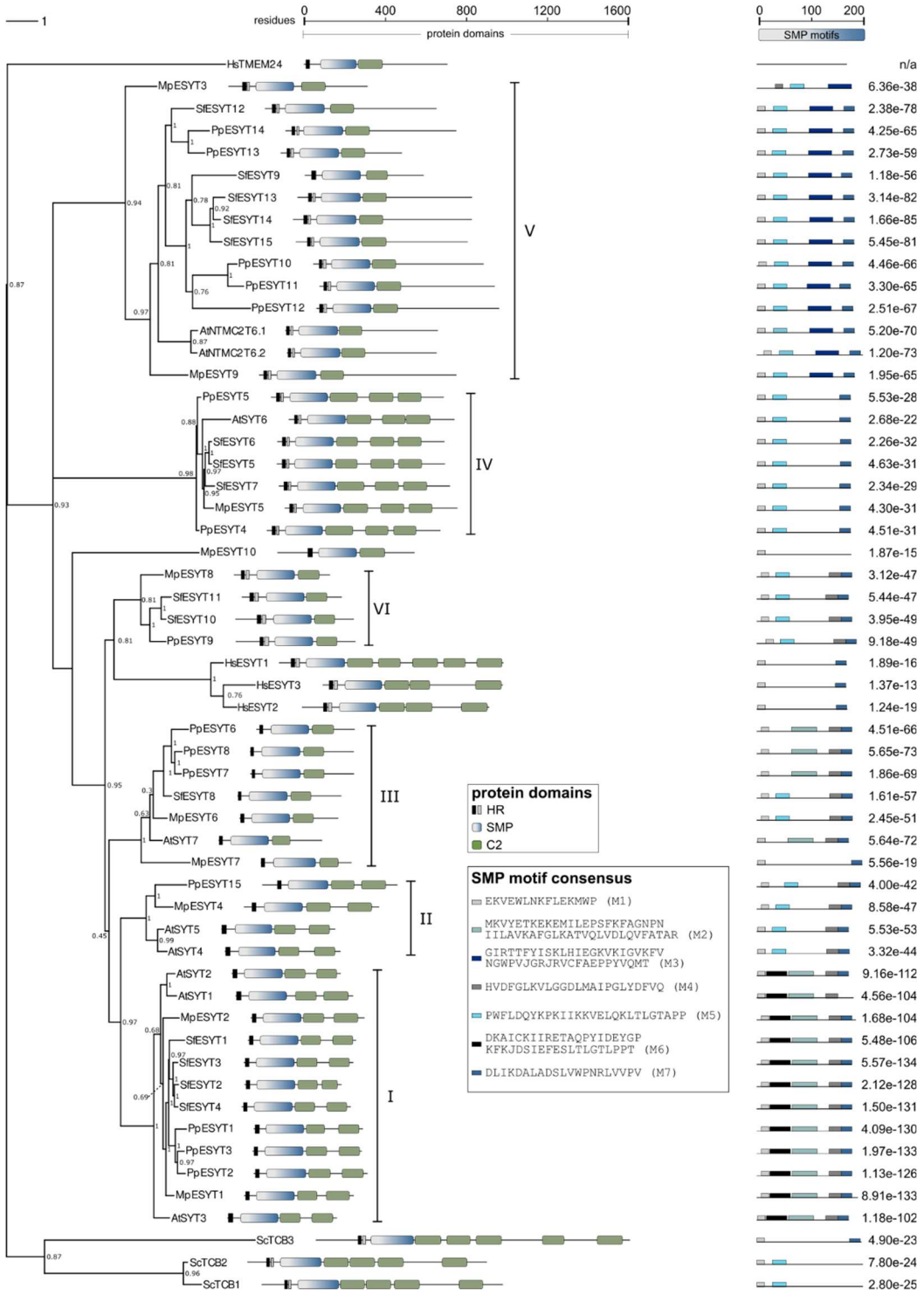

Figure 3. Phylogenetic tree of ESYT homologues. ESYT domain structure and overrepresented SMP motifs are shown. Protein sequences of ESYT homologues and HsTMEM24 of *H. sapiens* [44,64], *S. cerevisiae* [52], and *A. thaliana* [5,19,68] were reported previously. ESYT homologues of *P. patens*, *S. phallax* and *M. polymorpha* were identified using tBLASTn [112] (protein query against translated nucleotide databases) with genome databases deposited at Phytozome [113]. The phylogenetic tree was constructed by Maximum Likelihood and 1,000

 doi:10.20944/preprints202503.0048.v1

bootstrap iterations using the phangorn R package [114] (see Supplementary CodeS1.R for details). Bootstrap values are shown for the nodes. The branch length bar (upper left scale) represents the average number of substitutions per residue. For a tree containing branch lengths see Figure S2. The tree was edited using Inkscape [115]. Protein domains were identified using InterPro [116] and SMART [117] analyses. HR: hydrophobic region (black box, single HR; black and grey boxes, hairpin structure), SMP: Synaptotagmin-like Mitochondrial-lipid-binding Protein (grey-blue gradient box), C2: Ca^{2+}-dependent membrane-targeting domain (green box). SMP motifs M1–M7 (shades of grey and blue boxes) were identified using MEME [111], and the corresponding consensus sequences are displayed. Numbers adjacent to motifs depict the combined match p-value derived from the product of position p-values of the MEME output. Scales indicate amino acid residues of full-length sequences (upper middle scale) or SMP domains (upper right scale). HsTMEM24 could not be aligned in BLASTP or produce motifs in MEME analysis due to low homology to the other sequences, n/a: not applicable.

Based on the known functions of the AtSYT homologues present in classes I to IV and the close phylogenetic relationship to the bryophyte ESYTs identified in this study, physiological importance of the individual identified ESYTs may be hypothesized. The genes in class I could be involved in tip growth of protonemata and rhizoids, similar to the role of AtSYT1-2 in tip growth of pollen tubes and root hairs in Arabidopsis. Also, genes belonging to class I to IV may play a role in restoration of plasma membrane integration posterior to stress exposure as well as biotic stress response. Further, the genes belonging to class V, which also contains AtNTMC2T6.1 and AtNTMC2T6.2, have not yet been investigated regarding their biological function. Finally, since for the genes in class VI no orthologues has been identified in Arabidopsis according to our analysis, the function of these genes may differ from those observed in Arabidopsis so far.

3. Conclusions

This review presents a bioinformatic analysis of the ESYT gene family in the bryophyte *P. patens* and supports the findings by including two other bryophytes, *S. fallax* and *M. polymorpha*. The comparison of ESYTs in bryophytes with the angiosperm Arabidopsis revealed that all classes of ESYTs present in Arabidopsis did already exist in *P. patens*, which also contained an ESYT class with no counterpart in Arabidopsis. The results suggest that ESYTs have diverse functions in *P. patens* that could overlap with functions described in Arabidopsis in stress responses and may have contributed to the adaptation of the first land plants to terrestrial conditions. A potential functional diversity in the ESYT family of *P. patens* is further supported by the distribution of motifs in the SMP domains, which are shared with motifs in SMPs of Arabidopsis. *P. patens* is pointed out as an excellent model organism to examine ESYTs and the mechanisms underlying the formation and functions of MCSs. Due to the simple organization of its tissues, *P. patens* is especially suited to study the roles of ESYTs in tip growth and plasmodesmata development. The identification of conserved motifs in the SMP domain of plant-based ESYTs allows the formation of hypotheses regarding the mode of action ESYTs have within bryophytes. The same holds for the apparent variability in the number of C2 domains compared to animals and yeast, where ESYTs never occur with less than three C2 domains, which is apparently not true for plants. Future experiments are necessary to illuminate the roles of the genes and conserved motifs identified here in terms of their physiological and biochemical properties in this important model plant.

4. Methods

4.1. Genome and Protein Databases Search

The protein sequences of *H. sapiens* HsESYTs [44], HsTMEM24 [64] and *S. cerevisiae* ScTCBs [2,52] were obtained from the Universal Protein Resource (UniProt, https://www.uniprot.org/) [118]. ESYT homolog protein sequences AtSYTs and AtNTMC2T6s of Arabidopsis [5,19,30,68,69] were obtained from The Arabidopsis Information Resource (TAIR, https://www.arabidopsis.org/) [119]. ESYT homologues were identified in three model bryophytes for which complete annotated genome

 doi:10.20944/preprints202503.0048.v1

databases are available at the Phytozome (v13) depository (https://phytozome-next.jgi.doe.gov/) [113] using the genome database of *Physcomitrium patens* v6.1 (Phytozome genome ID:870) [102], *Sphagnum fallax* v1.1 (Phytozome genome ID: 522) [120] and *Marchantia polymorpha* v3.1 (Phytozome genome ID: 320) [121]. The data bases were searched using as queries the protein sequence of the full-length or the SMP domain of the following sequences: AtSYT1, AtSYT6, AtSYT7, AtNTMC2T6.1, HsESYT1, PpESYT1, PpESYT4, PpESYT10 (after PpESYT-like sequences were identified in *P. patens*) with the Protein Basic Local Alignment Search Tool (BLASTP) [112,122] applying default settings. Some ESYT homologues of *P. patens* and *M. polymorpha* were reported previously as indicated in Table S1 [19,70].

4.2. Protein Domains and Motif Analysis

The protein domains of HsTMEM24 and of ESYT homologues of *H sapiens*, *S. cerevisiae* and *A. thaliana* were reported previously [2,19,44,52,64,68]. The ESYTs of *P. patens*, *S. fallax* and *M. polymorpha* were analyzed using DeepTMHMM (v1.0) (https://dtu.biolib.com/DeepTMHMM) [123] for the prediction of hydrophobic regions. The Integrative Protein Signature Database (InterPro, https://www.ebi.ac.uk/interpro/) [116] and Simple Modular Architecture Research Tool (Smart BLAST, https://blast.ncbi.nlm.nih.gov/smartblast/) [117] were used for the prediction of protein domains. Only protein sequences with a predicted N-terminal hydrophobic region, an SMP domain and C2 domain(s) were used for further analyses (Table S1).

The reported and newly identified SMP domains were screened for motifs using MEME analysis (https://meme-suite.org/meme/) [111] applying the following settings: motif length 6 to 50 residues, motif occurrences in all sequences 2 to 56, maximum 1 motif occurrence per sequence maximum 10 motifs identified. The amino acid sequence of the identified motifs is displayed in Figure 4. The significance of the identified motifs was assessed with the combined match p-value, the probability that a random sequence of the same length would yield position p-values with a product smaller of equal to that of the tested sequence. A position p-value represents the likelihood of a random sequence matching the motif with a score equal or greater to the highest observed in the tested sequence.

4.3. Multiple Sequence Alignment and Phylogenetic Tree Construction

The 56 ESYT-like proteins of *H. sapiens*, *S. cerevisiae*, *A. thaliana*, *P. patens*, *S. fallax* and *M. polymorpha* were subjected to multiple sequence alignment (MSA), using the msa R package (v1.38.0) [124], specifying method='ClustalW' and the BLOSUM62 [125] substitution matrix. MSA results were visualized with the ggmsa function from the ggmsa R package (v1.12.0) [126,127] and protein domains were added using Inkscape [citation]. After alignment, a pairwise distance matrix was calculated using the dist.alignment function from the seqinr R package (v4.2-36) [128]. The phylogenetic tree was constructed using the maximum likelihood (ML) approach [110] as implemented in the phangorn R package (v2.12.1) [114]. Model selection was done using the modelTest function with all 17 available protein models. Inclusion or omission of invariant sites (+I) for completely conserved positions as well as well as a discrete gamma model (+G(4)) to account for different mutation rates throughout the alignment were tested separately as well as together. Finally, the Jones-Taylor-Thornton [129] model with consideration of invariant sites and varying mutation rates (JTT+G(4)+I) was selected for tree construction as it showed the lowest Bayesian Information Criterion (BIC) of all models with a value of 158957.4. The ML tree was calculated using the chosen model and the pml_bb function with 1,000 bootstrap iterations (rearrangement="stochastic"). All R code that was used for MSA, phylogenetic analyses and visualization is provided in the Supplementary CodeS1.R script.

Supplementary Materials: The following supporting information can be downloaded at: Preprints.org, TableS1: List of ESYT homologues used in this study. FigureS1: Multiple sequence alignment of all ESYTs. FigureS2: Phylogenetic tree of ESYTs with branch length distances. FigureS3: Heatmap of pairwise distances between

 doi:10.20944/preprints202503.0048.v1

ESYT sequences. CodeS1.R: R code used for multiple sequence alignment, calculation of phylogenetic tree and visualization of Figure 3 and Figures S1-S3.

Author Contributions: Conceptualization, M.N.; methodology, A.K. and M.N.; validation, A.K. and M.N.; formal analysis, A.K. and M.N.; writing—original draft preparation, A. K. and M.N.; writing—review and editing, A.K. and M.N.; visualization, A.K. and M.N.; supervision, M.N. All authors have read and agreed to the published version of the manuscript.

Funding This research received no funding.

Data Availability Statement: The original contributions presented in this study are included in the article/supplementary material. Further inquiries can be directed to the corresponding author.

Acknowledgments: We thank Lisa Koch for graphical support.

Conflicts of Interest: The authors declare no conflicts of interest.

References

1. Saheki, Y.; De Camilli, P. Endoplasmic Reticulum-Plasma Membrane Contact Sites. *Annu Rev Biochem* **2017**, *86*, 659-684. 10.1146/annurev-biochem-061516-044932
2. Toulmay, A.; Prinz, W.A. A conserved membrane-binding domain targets proteins to organelle contact sites. *Journal of Cell Science* **2012**, *125*, 49-58. 10.1242/jcs.085118
3. Giordano, F.; Saheki, Y.; Idevall-Hagren, O.; Colombo, S.F.; Pirruccello, M.; Milosevic, I.; Elena; Sviatoslav; Borgese, N.; De Camilli, P. PI(4,5)P2-Dependent and Ca2+-Regulated ER-PM Interactions Mediated by the Extended Synaptotagmins. *Cell* **2013**, *153*, 1494-1509. 10.1016/j.cell.2013.05.026
4. Saheki, Y.; De Camilli, P. The Extended-Synaptotagmins. *Biochimica et Biophysica Acta (BBA) - Molecular Cell Research* **2017**, *1864*, 1490-1493. doi.org/10.1016/j.bbamcr.2017.03.013
5. Schapire, A.L.; Voigt, B.; Jasik, J.; Rosado, A.; Lopez-Cobollo, R.; Menzel, D.; Salinas, J.; Mancuso, S.; Valpuesta, V.; Baluska, F.; et al. Arabidopsis synaptotagmin 1 is required for the maintenance of plasma membrane integrity and cell viability. *Plant Cell* **2008**, *20*, 3374-3388. 10.1105/tpc.108.063859
6. Benitez-Fuente, F.; Botella, M.A. Biological roles of plant synaptotagmins. *European Journal of Cell Biology* **2023**, *102*, 151335. doi.org/10.1016/j.ejcb.2023.151335
7. Grebnev, G.; Cvitkovic, M.; Fritz, C.; Cai, G.; Smith, A.-S.; Kost, B. Quantitative Structural Organization of Bulk Apical Membrane Traffic in Pollen Tubes. *Plant Physiology* **2020**, *183*, 1559-1585. 10.1104/pp.20.00380
8. Zhang, L.; Xing, J.; Lin, J. At the intersection of exocytosis and endocytosis in plants. *New Phytologist* **2019**, *224*, 1479-1489. doi.org/10.1111/nph.16018
9. Voeltz, G.K.; Sawyer, E.M.; Hajnóczky, G.; Prinz, W.A. Making the connection: How membrane contact sites have changed our view of organelle biology. *Cell* **2024**, *187*, 257-270. 10.1016/j.cell.2023.11.040
10. Bernhard, W.; Rouiller, C. Close topographical relationship between mitochondria and ergastoplasm of liver cells in a definite phase of cellular activity. *The Journal of Biophysical and Biochemical Cytology* **1956**, *2*, 73-78. 10.1083/jcb.2.4.73
11. Rosenbluth, J. Subsurface cisterns and their relationship to the neuronal plasma membrane. *Journal of Cell Biology* **1962**, *13*, 405-421. 10.1083/jcb.13.3.405
12. Lang, A.; John Peter, A.T.; Kornmann, B. ER–mitochondria contact sites in yeast: beyond the myths of ERMES. *Current Opinion in Cell Biology* **2015**, *35*, 7-12. doi.org/10.1016/j.ceb.2015.03.002
13. Phillips, M.J.; Voeltz, G.K. Structure and function of ER membrane contact sites with other organelles. *Nature Reviews Molecular Cell Biology* **2016**, *17*, 69-82. 10.1038/nrm.2015.8
14. Venditti, R.; Masone, M.C.; De Matteis, M.A. ER-Golgi membrane contact sites. *Biochemical Society Transactions* **2020**, *48*, 187-197. 10.1042/BST20190537
15. Renna, L.; Stefano, G.; Puggioni, M.P.; Kim, S.-J.; Lavell, A.; Froehlich, J.E.; Burkart, G.; Mancuso, S.; Benning, C.; Brandizzi, F. ER-associated VAP27-1 and VAP27-3 proteins functionally link the lipid-binding ORP2A at the ER-chloroplast contact sites. *Nature Communications* **2024**, *15*, 6008. 10.1038/s41467-024-50425-7

 doi:10.20944/preprints202503.0048.v1

16. Scorrano, L.; De Matteis, M.A.; Emr, S.; Giordano, F.; Hajnóczky, G.; Kornmann, B.; Lackner, L.L.; Levine, T.P.; Pellegrini, L.; Reinisch, K.; et al. Coming together to define membrane contact sites. *Nature Communications* **2019**, *10*, 1287. 10.1038/s41467-019-09253-3
17. Wu, M.M.; Buchanan, J.; Luik, R.M.; Lewis, R.S. Ca2+ store depletion causes STIM1 to accumulate in ER regions closely associated with the plasma membrane. *Journal of Cell Biology* **2006**, *174*, 803-813. 10.1083/jcb.200604014
18. Pérez-Sancho, J.; Vanneste, S.; Lee, E.; McFarlane, H.E.; Esteban del Valle, A.; Valpuesta, V.; Friml, J.; Botella, M.A.; Rosado, A. The Arabidopsis Synaptotagmin1 Is Enriched in Endoplasmic Reticulum-Plasma Membrane Contact Sites and Confers Cellular Resistance to Mechanical Stresses *Plant Physiology* **2015**, *168*, 132-143. 10.1104/pp.15.00260
19. Ishikawa, K.; Tamura, K.; Fukao, Y.; Shimada, T. Structural and functional relationships between plasmodesmata and plant endoplasmic reticulum–plasma membrane contact sites consisting of three synaptotagmins. *New Phytologist* **2020**, *226*, 798-808. 10.1111/nph.16391
20. Hoffmann, P.C.; Bharat, T.A.M.; Wozny, M.R.; Boulanger, J.; Miller, E.A.; Kukulski, W. Tricalbins Contribute to Cellular Lipid Flux and Form Curved ER-PM Contacts that Are Bridged by Rod-Shaped Structures. *Developmental Cell* **2019**, *51*, 488-502.e488. doi.org/10.1016/j.devcel.2019.09.019
21. Wang, P.; Hawkins, Timothy J.; Richardson, C.; Cummins, I.; Deeks, Michael J.; Sparkes, I.; Hawes, C.; Hussey, Patrick J. The Plant Cytoskeleton, NET3C, and VAP27 Mediate the Link between the Plasma Membrane and Endoplasmic Reticulum. *Current Biology* **2014**, *24*, 1397-1405. 10.1016/j.cub.2014.05.003
22. Peretti, D.; Dahan, N.; Shimoni, E.; Hirschberg, K.; Lev, S. Coordinated Lipid Transfer between the Endoplasmic Reticulum and the Golgi Complex Requires the VAP Proteins and Is Essential for Golgi-mediated Transport. *Molecular Biology of the Cell* **2008**, *19*, 3871-3884. 10.1091/mbc.e08-05-0498
23. Ye, H.; Gao, J.; Liang, Z.; Lin, Y.; Yu, Q.; Huang, S.; Jiang, L. Arabidopsis ORP2A mediates ER–autophagosomal membrane contact sites and regulates PI3P in plant autophagy. *Proceedings of the National Academy of Sciences* **2022**, *119*, e2205314119. 10.1073/pnas.2205314119
24. Rocha, N.; Kuijl, C.; van der Kant, R.; Janssen, L.; Houben, D.; Janssen, H.; Zwart, W.; Neefjes, J. Cholesterol sensor ORP1L contacts the ER protein VAP to control Rab7–RILP–p150Glued and late endosome positioning. *Journal of Cell Biology* **2009**, *185*, 1209-1225. 10.1083/jcb.200811005
25. Wang, P.; Richardson, C.; Hawkins, T.J.; Sparkes, I.; Hawes, C.; Hussey, P.J. Plant VAP27 proteins: domain characterization, intracellular localization and role in plant development. *New Phytologist* **2016**, *210*, 1311-1326. doi.org/10.1111/nph.13857
26. Zang, J.; Klemm, S.; Pain, C.; Duckney, P.; Bao, Z.; Stamm, G.; Kriechbaumer, V.; Bürstenbinder, K.; Hussey, P.J.; Wang, P. A novel plant actin-microtubule bridging complex regulates cytoskeletal and ER structure at ER-PM contact sites. *Current Biology* **2021**, *31*, 1251-1260.e1254. doi.org/10.1016/j.cub.2020.12.009
27. Friedman, J.R.; Lackner, L.L.; West, M.; DiBenedetto, J.R.; Nunnari, J.; Voeltz, G.K. ER tubules mark sites of mitochondrial division. *Science* **2011**, *334*, 358-362. 10.1126/science.1207385
28. Ji, W.-K.; Chakrabarti, R.; Fan, X.; Schoenfeld, L.; Strack, S.; Higgs, H.N. Receptor-mediated Drp1 oligomerization on endoplasmic reticulum. *Journal of Cell Biology* **2017**, *216*, 4123-4139. 10.1083/jcb.201610057
29. Li, C.; Duckney, P.; Zhang, T.; Fu, Y.; Li, X.; Kroon, J.; De Jaeger, G.; Cheng, Y.; Hussey, P.J.; Wang, P. TraB family proteins are components of ER-mitochondrial contact sites and regulate ER-mitochondrial interactions and mitophagy. *Nat Commun* **2022**, *13*, 5658. 10.1038/s41467-022-33402-w
30. Ruiz-Lopez, N.; Pérez-Sancho, J.; del Valle, A.E.; Haslam, R.P.; Vanneste, S.; Catalá, R.; Perea-Resa, C.; Damme, D.V.; García-Hernández, S.; Albert, A.; et al. Synaptotagmins at the endoplasmic reticulum–plasma membrane contact sites maintain diacylglycerol homeostasis during abiotic stress. *The Plant Cell* **2021**, *33*, 2431-2453. 10.1093/plcell/koab122
31. Reinisch, K.M.; Prinz, W.A. Mechanisms of nonvesicular lipid transport. *Journal of Cell Biology* **2021**, *220*, e202012058. 10.1083/jcb.202012058
32. Roos, J.; DiGregorio, P.J.; Yeromin, A.V.; Ohlsen, K.; Lioudyno, M.; Zhang, S.; Safrina, O.; Kozak, J.A.; Wagner, S.L.; Cahalan, M.D.; et al. STIM1, an essential and conserved component of store-operated Ca2+ channel function. *Journal of Cell Biology* **2005**, *169*, 435-445. 10.1083/jcb.200502019

 doi:10.20944/preprints202503.0048.v1

33. Yeromin, A.V.; Zhang, S.L.; Jiang, W.; Yu, Y.; Safrina, O.; Cahalan, M.D. Molecular identification of the CRAC channel by altered ion selectivity in a mutant of Orai. *Nature* **2006**, *443*, 226-229. 10.1038/nature05108
34. Vig, M.; Peinelt, C.; Beck, A.; Koomoa, D.L.; Rabah, D.; Koblan-Huberson, M.; Kraft, S.; Turner, H.; Fleig, A.; Penner, R.; et al. CRACM1 Is a Plasma Membrane Protein Essential for Store-Operated Ca2+ Entry. *Science* **2006**, *312*, 1220-1223. 10.1126/science.1127883
35. Prakriya, M.; Feske, S.; Gwack, Y.; Srikanth, S.; Rao, A.; Hogan, P.G. Orai1 is an essential pore subunit of the CRAC channel. *Nature* **2006**, *443*, 230-233. 10.1038/nature05122
36. Putney, J.W. A model for receptor-regulated calcium entry. *Cell Calcium* **1986**, *7*, 1-12. doi.org/10.1016/0143-4160(86)90026-6
37. Coussens, L.; Parker, P.J.; Rhee, L.; Yang-Feng, T.L.; Chen, E.; Waterfield, M.D.; Francke, U.; Ullrich, A. Multiple, Distinct Forms of Bovine and Human Protein Kinase C Suggest Diversity in Cellular Signaling Pathways. *Science* **1986**, *233*, 859-866. 10.1126/science.3755548
38. Matthew, W.D.; Tsavaler, L.; Reichardt, L.F. Identification of a synaptic vesicle-specific membrane protein with a wide distribution in neuronal and neurosecretory tissue. *Journal of Cell Biology* **1981**, *91*, 257-269. 10.1083/jcb.91.1.257
39. Chapman, E.R. How Does Synaptotagmin Trigger Neurotransmitter Release? *Annual Review of Biochemistry* **2008**, *77*, 615-641. 10.1146/annurev.biochem.77.062005.101135
40. Tang, J.; Maximov, A.; Shin, O.-H.; Dai, H.; Rizo, J.; Südhof, T.C. A Complexin/Synaptotagmin 1 Switch Controls Fast Synaptic Vesicle Exocytosis. *Cell* **2006**, *126*, 1175-1187. 10.1016/j.cell.2006.08.030
41. Brose, N.; Petrenko, A.G.; Südhof, T.C.; Jahn, R. Synaptotagmin: a Calcium Sensor on the Synaptic Vesicle Surface. *Science* **1992**, *256*, 1021-1025. 10.1126/science.1589771
42. Perin, M.S.; Fried, V.A.; Mignery, G.A.; Jahn, R.; Südhof, T.C. Phospholipid binding by a synaptic vesicle protein homologous to the regulatory region of protein kinase C. *Nature* **1990**, *345*, 260-263. 10.1038/345260a0
43. Sugita, S.; Shin, O.H.; Han, W.; Lao, Y.; Südhof, T.C. Synaptotagmins form a hierarchy of exocytotic Ca(2+) sensors with distinct Ca(2+) affinities. *Embo j* **2002**, *21*, 270-280. 10.1093/emboj/21.3.270
44. Min, S.-W.; Chang, W.-P.; Südhof, T.C. E-Syts, a family of membranous Ca 2+-sensor proteins with multiple C2 domains. *Proceedings of the National Academy of Sciences* **2007**, *104*, 3823-3828. 10.1073/pnas.0611725104
45. Lee, I.; Hong, W. Diverse membrane-associated proteins contain a novel SMP domain. *The FASEB Journal* **2006**, *20*, 202-206. doi.org/10.1096/fj.05-4581hyp
46. Schauder, C.M.; Wu, X.; Saheki, Y.; Narayanaswamy, P.; Torta, F.; Wenk, M.R.; De Camilli, P.; Reinisch, K.M. Structure of a lipid-bound extended synaptotagmin indicates a role in lipid transfer. *Nature* **2014**, *510*, 552-555. 10.1038/nature13269
47. Levine, T.P. Remote homology searches identify bacterial homologues of eukaryotic lipid transfer proteins, including Chorein-N domains in TamB and AsmA and Mdm31p. *BMC Molecular and Cell Biology* **2019**, *20*, 43. 10.1186/s12860-019-0226-z
48. Ge, J.; Bian, X.; Ma, L.; Cai, Y.; Li, Y.; Yang, J.; Karatekin, E.; De Camilli, P.; Zhang, Y. Stepwise membrane binding of extended synaptotagmins revealed by optical tweezers. *Nature Chemical Biology* **2022**, *18*, 313-320. 10.1038/s41589-021-00914-3
49. Saheki, Y.; Bian, X.; Schauder, C.M.; Sawaki, Y.; Surma, M.A.; Klose, C.; Pincet, F.; Reinisch, K.M.; De Camilli, P. Control of plasma membrane lipid homeostasis by the extended synaptotagmins. *Nature Cell Biology* **2016**, *18*, 504-515. 10.1038/ncb3339
50. Wang, Y.; Li, Z.; Wang, X.; Zhao, Z.; Jiao, L.; Liu, R.; Wang, K.; Ma, R.; Yang, Y.; Chen, G.; et al. Insights into membrane association of the SMP domain of extended synaptotagmin. *Nature Communications* **2023**, *14*, 1504. 10.1038/s41467-023-37202-8
51. Ishikawa, K.; Tamura, K.; Ueda, H.; Ito, Y.; Nakano, A.; Hara-Nishimura, I.; Shimada, T. Synaptotagmin-Associated Endoplasmic Reticulum-Plasma Membrane Contact Sites Are Localized to Immobile ER Tubules. *Plant Physiol* **2018**, *178*, 641-653. 10.1104/pp.18.00498
52. Manford, A., G.; Stefan, C., J.; Yuan, H., L. ; MacGurn, J., A.; Emr, S., D. . ER-to-Plasma Membrane Tethering Proteins Regulate Cell Signaling and ER Morphology. *Developmental Cell* **2012**, *23*, 1129-1140. 10.1016/j.devcel.2012.11.004

 doi:10.20944/preprints202503.0048.v1

53. Benavente, J.L.; Siliqi, D.; Infantes, L.; Lagartera, L.; Mills, A.; Gago, F.; Ruiz-López, N.; Botella, M.A.; Sánchez-Barrena, M.J.; Albert, A. The structure and flexibility analysis of the Arabidopsis synaptotagmin 1 reveal the basis of its regulation at membrane contact sites. *Life Science Alliance* **2021**, *4*, e202101152. 10.26508/lsa.202101152
54. Yu, H.; Liu, Y.; Gulbranson, D.R.; Paine, A.; Rathore, S.S.; Shen, J. Extended synaptotagmins are Ca2+-dependent lipid transfer proteins at membrane contact sites. *Proc Natl Acad Sci U S A* **2016**, *113*, 4362-4367. 10.1073/pnas.1517259113
55. Fernández-Busnadiego, R.; Saheki, Y.; De Camilli, P. Three-dimensional architecture of extended synaptotagmin-mediated endoplasmic reticulum–plasma membrane contact sites. *Proceedings of the National Academy of Sciences* **2015**, *112*, E2004-E2013. 10.1073/pnas.1503191112
56. Yamazaki, T.; Takata, N.; Uemura, M.; Kawamura, Y. Arabidopsis synaptotagmin SYT1, a type I signal-anchor protein, requires tandem C2 domains for delivery to the plasma membrane. *J Biol Chem* **2010**, *285*, 23165-23176. 10.1074/jbc.M109.084046
57. Idevall-Hagren, O.; Lü, A.; Xie, B.; De Camilli, P. Triggered Ca2+ influx is required for extended synaptotagmin 1-induced ER-plasma membrane tethering. *The EMBO Journal* **2015**, *34*, 2291-2305-2305. doi.org/10.15252/embj.201591565
58. Xu, J.; Bacaj, T.; Zhou, A.; Tomchick, Diana R.; Südhof, Thomas C.; Rizo, J. Structure and Ca2+ Binding Properties of the Tandem C2 Domains of E-Syt2. *Structure* **2014**, *22*, 269-280. 10.1016/j.str.2013.11.011
59. von Poser, C.; Ichtchenko, K.; Shao, X.; Rizo, J.; Südhof, T.C. The evolutionary pressure to inactivate: a subclass of Synaptotagmins with an amino acid substitution that abolishes Ca2+ binding. *Journal of Biological Chemistry* **1997**, *272*, 14314-14319. doi.org/10.1074/jbc.272.22.14314
60. Yamazaki, T.; Kawamura, Y.; Minami, A.; Uemura, M. Calcium-dependent freezing tolerance in Arabidopsis involves membrane resealing via synaptotagmin SYT1. *Plant Cell* **2008**, *20*, 3389-3404. 10.1105/tpc.108.062679
61. Bian, X.; Saheki, Y.; De Camilli, P. Ca(2+) releases E-Syt1 autoinhibition to couple ER-plasma membrane tethering with lipid transport. *Embo J* **2018**, *37*, 219-234. 10.15252/embj.201797359
62. Davletov, B.A.; Südhof, T.C. A single C2 domain from synaptotagmin I is sufficient for high affinity Ca2+/phospholipid binding. *J Biol Chem* **1993**, *268*, 26386-26390.
63. Gruget, C.; Bello, O.; Coleman, J.; Krishnakumar, S.S.; Perez, E.; Rothman, J.E.; Pincet, F.; Donaldson, S.H. Synaptotagmin-1 membrane binding is driven by the C2B domain and assisted cooperatively by the C2A domain. *Scientific Reports* **2020**, *10*, 18011. 10.1038/s41598-020-74923-y
64. Lees, J.A.; Messa, M.; Sun, E.W.; Wheeler, H.; Torta, F.; Wenk, M.R.; De Camilli, P.; Reinisch, K.M. Lipid transport by TMEM24 at ER-plasma membrane contacts regulates pulsatile insulin secretion. *Science* **2017**, *355*, 10.1126/science.aah6171
65. Pottekat, A.; Becker, S.; Spencer, Kathryn R.; Yates, John R.; Manning, G.; Itkin-Ansari, P.; Balch, William E. Insulin Biosynthetic Interaction Network Component, TMEM24, Facilitates Insulin Reserve Pool Release. *Cell Reports* **2013**, *4*, 921-930. doi.org/10.1016/j.celrep.2013.07.050
66. Sun, E.W.; Guillén-Samander, A.; Bian, X.; Wu, Y.; Cai, Y.; Messa, M.; De Camilli, P. Lipid transporter TMEM24/C2CD2L is a Ca(2+)-regulated component of ER-plasma membrane contacts in mammalian neurons. *Proc Natl Acad Sci U S A* **2019**, *116*, 5775-5784. 10.1073/pnas.1820156116
67. Xie, B.; Panagiotou, S.; Cen, J.; Gilon, P.; Bergsten, P.; Idevall-Hagren, O. The endoplasmic reticulum-plasma membrane tethering protein TMEM24 is a regulator of cellular Ca2+ homeostasis. *J Cell Sci* **2021**, *135*, 10.1242/jcs.259073
68. Huercano, C.; Percio, F.; Sanchez-Vera, V.; Morello-López, J.; Botella, M.A.; Ruiz-Lopez, N. Identification of plant exclusive lipid transfer SMP proteins at membrane contact sites in Arabidopsis and Tomato. *bioRxiv* **2022**, 2022.2012.2014.520452. 10.1101/2022.12.14.520452
69. Lee, E.; Santana, B.V.N.; Samuels, E.; Benitez-Fuente, F.; Corsi, E.; Botella, M.A.; Perez-Sancho, J.; Vanneste, S.; Friml, J.; Macho, A.; et al. Rare earth elements induce cytoskeleton-dependent and PI4P-associated rearrangement of SYT1/SYT5 endoplasmic reticulum–plasma membrane contact site complexes in Arabidopsis. *Journal of Experimental Botany* **2020**, *71*, 3986-3998. 10.1093/jxb/eraa138

 doi:10.20944/preprints202503.0048.v1

70. Craxton, M. Evolutionary genomics of plant genes encoding N-terminal-TM-C2 domain proteins and the similar FAM62 genes and synaptotagmin genes of metazoans. *BMC Genomics* **2007**, *8*, 259. 10.1186/1471-2164-8-259
71. Lee, E.; Vanneste, S.; Pérez-Sancho, J.; Benitez-Fuente, F.; Strelau, M.; Macho, A.P.; Botella, M.A.; Friml, J.; Rosado, A. Ionic stress enhances ER-PM connectivity via phosphoinositide-associated SYT1 contact site expansion in Arabidopsis. *Proc Natl Acad Sci U S A* **2019**, *116*, 1420-1429. 10.1073/pnas.1818099116
72. García-Hernández, S.; Rubio, L.; Pérez-Sancho, J.; Esteban del Valle, A.; Benítez-Fuente, F.; Beuzón, C.R.; Macho, A.P.; Ruiz-López, N.; Albert, A.; Botella, M.A. Unravelling Different Biological Roles Of Plant Synaptotagmins. *bioRxiv* **2024**, 2024.2001.2021.576508. 10.1101/2024.01.21.576508
73. Kumar, A.; Krausko, M.; Jásik, J. SYNAPTOTAGMIN 4 is expressed mainly in the phloem and participates in abiotic stress tolerance in Arabidopsis. *Frontiers in Plant Science* **2024**, *15*,
74. Wang, H.; Han, S.; Siao, W.; Song, C.; Xiang, Y.; Wu, X.; Cheng, P.; Li, H.; Jásik, J.; Mičieta, K.; et al. Arabidopsis Synaptotagmin 2 Participates in Pollen Germination and Tube Growth and Is Delivered to Plasma Membrane via Conventional Secretion. *Molecular Plant* **2015**, *8*, 1737-1750. 10.1016/j.molp.2015.09.003
75. Zhang, H.; Zhang, L.; Gao, B.; Fan, H.; Jin, J.; Botella, M.A.; Jiang, L.; Lin, J. Golgi Apparatus-Localized Synaptotagmin 2 Is Required for Unconventional Secretion in Arabidopsis. *PLoS ONE* **2011**, *6*, e26477. 10.1371/journal.pone.0026477
76. Kwon, C.; Neu, C.; Pajonk, S.; Yun, H.S.; Lipka, U.; Humphry, M.; Bau, S.; Straus, M.; Kwaaitaal, M.; Rampelt, H.; et al. Co-option of a default secretory pathway for plant immune responses. *Nature* **2008**, *451*, 835-840. 10.1038/nature06545
77. Cabanillas, D.G.; Jiang, J.; Movahed, N.; Germain, H.; Yamaji, Y.; Zheng, H.; Laliberté, J.F. Turnip Mosaic Virus Uses the SNARE Protein VTI11 in an Unconventional Route for Replication Vesicle Trafficking. *Plant Cell* **2018**, *30*, 2594-2615. 10.1105/tpc.18.00281
78. Siao, W.; Wang, P.; Voigt, B.; Hussey, P.J.; Baluska, F. Arabidopsis SYT1 maintains stability of cortical endoplasmic reticulum networks and VAP27-1-enriched endoplasmic reticulum-plasma membrane contact sites. *J Exp Bot* **2016**, *67*, 6161-6171. 10.1093/jxb/erw381
79. Creutz, C.E.; Snyder, S.L.; Schulz, T.A. Characterization of the yeast tricalbins: membrane-bound multi-C2-domain proteins that form complexes involved in membrane trafficking. *Cellular and Molecular Life Sciences CMLS* **2004**, *61*, 1208-1220. 10.1007/s00018-004-4029-8
80. Codjoe, J.M.; Richardson, R.A.; McLoughlin, F.; Vierstra, R.D.; Haswell, E.S. Unbiased proteomic and forward genetic screens reveal that mechanosensitive ion channel MSL10 functions at ER–plasma membrane contact sites in Arabidopsis thaliana. *eLife* **2022**, *11*, 10.7554/elife.80501
81. Basu, D.; Haswell, E.S. The Mechanosensitive Ion Channel MSL10 Potentiates Responses to Cell Swelling in Arabidopsis Seedlings. *Current Biology* **2020**, *30*, 2716-2728.e2716. doi.org/10.1016/j.cub.2020.05.015
82. Kang, F.; Zhou, M.; Huang, X.; Fan, J.; Wei, L.; Boulanger, J.; Liu, Z.; Salamero, J.; Liu, Y.; Chen, L. E-syt1 Re-arranges STIM1 Clusters to Stabilize Ring-shaped ER-PM Contact Sites and Accelerate Ca(2+) Store Replenishment. *Sci Rep* **2019**, *9*, 3975. 10.1038/s41598-019-40331-0
83. Qian, T.; Li, C.; Liu, F.; Xu, K.; Wan, C.; Liu, Y.; Yu, H. Arabidopsis synaptotagmin 1 mediates lipid transport in a lipid composition-dependent manner. *Traffic* **2022**, *23*, 346-356. 10.1111/tra.12844
84. Bell, K.; Oparka, K. Imaging plasmodesmata. *Protoplasma* **2011**, *248*, 9-25. 10.1007/s00709-010-0233-6
85. Bayer, E.M.; Benitez-Alfonso, Y. Plasmodesmata: Channels Under Pressure. *Annual Review of Plant Biology 75*, 291-317. doi.org/10.1146/annurev-arplant-070623-093110
86. Robertson, J.D.; Locke, M. Cellular membranes in development. *by M. Locke, Academic Press, Inc., New York* **1964**, 1.
87. Brault, M.L.; Petit, J.D.; Immel, F.; Nicolas, W.J.; Glavier, M.; Brocard, L.; Gaston, A.; Fouché, M.; Hawkins, T.J.; Crowet, J.M.; et al. Multiple C2 domains and transmembrane region proteins (MCTPs) tether membranes at plasmodesmata. *EMBO reports* **2019**, *20*, 10.15252/embr.201847182
88. Kriechbaumer, V.; Botchway, S.W.; Slade, S.E.; Knox, K.; Frigerio, L.; Oparka, K.; Hawes, C. Reticulomics: Protein-Protein Interaction Studies with Two Plasmodesmata-Localized Reticulon Family Proteins Identify

 doi:10.20944/preprints202503.0048.v1

Binding Partners Enriched at Plasmodesmata, Endoplasmic Reticulum, and the Plasma Membrane. *Plant Physiol* **2015**, *169*, 1933-1945. 10.1104/pp.15.01153

89. Kim, S.; Park, K.; Kwon, C.; Yun, H.S. Synaptotagmin 4 and 5 additively contribute to Arabidopsis immunity to Pseudomonas syringae DC3000. *Plant Signal Behav* **2022**, *17*, 2025323. 10.1080/15592324.2021.2025323
90. Rensing, S.A.; Goffinet, B.; Meyberg, R.; Wu, S.-Z.; Bezanilla, M. The Moss *Physcomitrium* (*Physcomitrella*) *patens*: A Model Organism for Non-Seed Plants. *Plant Cell* **2020**, *32*, 1361-1376. doi.org/10.1105/tpc.19.00828
91. Menand, B.; Calder, G.; Dolan, L. Both chloronemal and caulonemal cells expand by tip growth in the moss *Physcomitrella patens*. *Journal of Experimental Botany* **2007**, *58*, 1843-1849. doi.org/10.1093/jxb/erm047
92. Jang, G.; Dolan, L. Auxin promotes the transition from chloronema to caulonema in moss protonema by positively regulating PpRSL1and PpRSL2 in *Physcomitrella patens*. *New Phytol.* **2011**, *192*, 319-327. doi.org/10.1111/j.1469-8137.2011.03805.x
93. Thelander, M.; Landberg, K.; Sundberg, E. Auxin-mediated developmental control in the moss Physcomitrella patens. *Journal of Experimental Botany* **2018**, *69*, 277-290.
94. Ntefidou, M.; Eklund, D.M.; Le Bail, A.; Schulmeister, S.; Scherbel, F.; Brandl, L.; Dörfler, W.; Eichstädt, C.; Bannmüller, A.; Ljung, K.; et al. *Physcomitrium patens* PpRIC, an ancestral CRIB-domain ROP effector, inhibits auxin-induced differentiation of apical initial cells. *Cell Rep.* **2023**, *42*, doi.org/10.1016/j.celrep.2023.112130
95. Jaeger, R.; Moody, L.A. A fundamental developmental transition in *Physcomitrium patens* is regulated by evolutionarily conserved mechanisms. *Evol. Devel.* **2021**, *23*, 123-136. doi.org/10.1111/ede.12376
96. Thelander, M.; Olsson, T.; Ronne, H. Effect of the energy supply on filamentous growth and development in *Physcomitrella patens*. *J. Exp. Bot.* **2005**, *56*, 653-662. 10.1093/jxb/eri040
97. Schumaker, K.S.; Dietrich, M.A. Programmed Changes in Form during Moss Development. *Plant Cell* **1997**, *9*, 1099-1107. doi.org/10.1105/tpc.9.7.1099
98. Hata, Y.; Ohtsuka, J.; Hiwatashi, Y.; Naramoto, S.; Kyozuka, J. Cytokinin and ALOG proteins regulate pluripotent stem cell identity in the moss Physcomitrium patens. *Science Advances* **2024**, *10*, eadq6082. 10.1126/sciadv.adq6082
99. Schulz, P.; Reski, R.; Maldiney, R.; Laloue, M.; Schwartzenberg, K.v. Kinetics of Cytokinin Production and Bud Formation in Physcomitrella: Analysis of Wild Type, a Developmental Mutant and Two of Its ipt Transgenics. *Journal of Plant Physiology* **2000**, *156*, 768-774. doi.org/10.1016/S0176-1617(00)80246-1
100. Moody, L.A.; Kelly, S.; Rabbinowitsch, E.; Langdale, J.A. Genetic Regulation of the 2D to 3D Growth Transition in the Moss *Physcomitrella patens*. *Curr. Biol.* **2018**, *28*, 473-478.e475. doi.org/10.1016/j.cub.2017.12.052
101. Jones, V.A.S.; Dolan, L. The evolution of root hairs and rhizoids. *Annals of Botany* **2012**, *110*, 205-212. 10.1093/aob/mcs136
102. Bi, G.; Zhao, S.; Yao, J.; Wang, H.; Zhao, M.; Sun, Y.; Hou, X.; Haas, F.B.; Varshney, D.; Prigge, M.; et al. Near telomere-to-telomere genome of the model plant Physcomitrium patens. *Nat. Plants* **2024**, *10*, 327-343. doi.org/10.1038/s41477-023-01614-7
103. Brunkard, J.O.; Zambryski, P.C. Plasmodesmata enable multicellularity: new insights into their evolution, biogenesis, and functions in development and immunity. *Current Opinion in Plant Biology* **2017**, *35*, 76-83. doi.org/10.1016/j.pbi.2016.11.007
104. Cook, M.E.; Graham, L.E.; Botha, C.E.J.; Lavin, C.A. Comparative ultrastructure of plasmodesmata of Chara and selected bryophytes: toward an elucidation of the evolutionary origin of plant plasmodesmata. *American Journal of Botany* **1997**, *84*, 1169-1178. doi.org/10.2307/2446040
105. Wegner, L.; Ehlers, K. Plasmodesmata dynamics in bryophyte model organisms: secondary formation and developmental modifications of structure and function. *Planta* **2024**, *260*, 45. 10.1007/s00425-024-04476-1
106. Olsson, T.; Thelander, M.; Ronne, H. A Novel Type of Chloroplast Stromal Hexokinase Is the Major Glucose-phosphorylating Enzyme in the Moss Physcomitrella patens. *Journal of Biological Chemistry* **2003**, *278*, 44439-44447. 10.1074/jbc.m306265200

107. Rensing, S.A.; Lang, D.; Zimmer, A.D.; Terry, A.; Salamov, A.; Shapiro, H.; Nishiyama, T.; Perroud, P.-F.O.; Lindquist, E.A.; Kamisugi, Y.; et al. The Physcomitrella genome reveals evolutionary insights into the conquest of land by plants. *Science* **2008**, *319*, 64-69. 10.1126/science.1150646
108. Schreiber, M.; Rensing, S.A.; Gould, S.B. The greening ashore. *Trends in Plant Science* **2022**, *27*, 847-857. doi.org/10.1016/j.tplants.2022.05.005
109. Hori, K.; Maruyama, F.; Fujisawa, T.; Togashi, T.; Yamamoto, N.; Seo, M.; Sato, S.; Yamada, T.; Mori, H.; Tajima, N.; et al. Klebsormidium flaccidum genome reveals primary factors for plant terrestrial adaptation. *Nature Communications* **2014**, *5*, 3978. 10.1038/ncomms4978
110. Felsenstein, J. Evolutionary trees from DNA sequences: a maximum likelihood approach. *J Mol Evol* **1981**, *17*, 368-376. 10.1007/bf01734359
111. Bailey, T.L.; Johnson, J.; Grant, C.E.; Noble, W.S. The MEME Suite. *Nucleic Acids Research* **2015**, *43*, W39-W49. 10.1093/nar/gkv416
112. Altschul, S.F.; Gish, W.; Miller, W.; Myers, E.W.; Lipman, D.J. Basic local alignment search tool. *J. Mol. Biol.* **1990**, *215*, 403-410. doi.org/10.1016/S0022-2836(05)80360-2
113. Goodstein, D.M.; Shu, S.; Howson, R.; Neupane, R.; Hayes, R.D.; Fazo, J.; Mitros, T.; Dirks, W.; Hellsten, U.; Putnam, N.; et al. Phytozome: a comparative platform for green plant genomics. *Nucleic Acids Res.* **2012**, *40*, D1178-D1186. doi.org/10.1093/nar/gkr944
114. Schliep, K.P. phangorn: phylogenetic analysis in R. *Bioinformatics* **2011**, *27*, 592-593. 10.1093/bioinformatics/btq706
115. Project, I. Inkscape. **2020**, doi: DOI.
116. Blum, M.; Andreeva, A.; Florentino, Laise C.; Chuguransky, Sara R.; Grego, T.; Hobbs, E.; Pinto, Beatriz L.; Orr, A.; Paysan-Lafosse, T.; Ponamareva, I.; et al. InterPro: the protein sequence classification resource in 2025. *Nucleic Acids Research* **2025**, *53*, D444-D456. 10.1093/nar/gkae1082
117. Letunic, I.; Khedkar, S.; Bork, P. SMART: recent updates, new developments and status in 2020. *Nucleic Acids Research* **2021**, *49*, D458-D460. 10.1093/nar/gkaa937
118. The UniProt Consortium. UniProt: the Universal Protein Knowledgebase in 2025. *Nucleic Acids Res.* **2024**, gkae1010. doi.org/10.1093/nar/gkae1010
119. Berardini, T.Z.; Reiser, L.; Li, D.; Mezheritsky, Y.; Muller, R.; Strait, E.; Huala, E. The arabidopsis information resource: Making and mining the "gold standard" annotated reference plant genome. *genesis* **2015**, *53*, 474-485. doi.org/10.1002/dvg.22877
120. Healey, A.L.; Piatkowski, B.; Lovell, J.T.; Sreedasyam, A.; Carey, S.B.; Mamidi, S.; Shu, S.; Plott, C.; Jenkins, J.; Lawrence, T.; et al. Newly identified sex chromosomes in the Sphagnum (peat moss) genome alter carbon sequestration and ecosystem dynamics. *Nature Plants* **2023**, *9*, 238-254. 10.1038/s41477-022-01333-5
121. Bowman, J.L.; Kohchi, T.; Yamato, K.T.; Jenkins, J.; Shu, S.; Ishizaki, K.; Yamaoka, S.; Nishihama, R.; Nakamura, Y.; Berger, F.; et al. Insights into Land Plant Evolution Garnered from the Marchantia polymorpha Genome. *Cell* **2017**, *171*, 287-304.e215. doi.org/10.1016/j.cell.2017.09.030
122. Camacho, C.; Coulouris, G.; Avagyan, V.; Ma, N.; Papadopoulos, J.; Bealer, K.; Madden, T.L. BLAST+: architecture and applications. *BMC Bioinformatics* **2009**, *10*, 421. 10.1186/1471-2105-10-421
123. Hallgren, J.; Tsirigos, K.; Pedersen, M.D.; Almagro Armenteros, J.J.; Marcatili, P.; Nielsen, H.; Krogh, A.; Winther, O. DeepTMHMM predicts alpha and beta transmembrane proteins using deep neural networks. *bioRxiv* **2022**, 10.1101/2022.04.08.487609
124. Bodenhofer, U.; Bonatesta, E.; Horejš-Kainrath, C.; Hochreiter, S. msa: an R package for multiple sequence alignment. *Bioinformatics* **2015**, *31*, 3997-3999. 10.1093/bioinformatics/btv494
125. Henikoff, S.; Henikoff, J.G. Amino acid substitution matrices from protein blocks. *Proceedings of the National Academy of Sciences* **1992**, *89*, 10915-10919. 10.1073/pnas.89.22.10915
126. Yu, G. *Data Integration, Manipulation and Visualization of Phylogenetic Trees*; CRC Press, Taylor & Francis Group: New York, 2022.
127. Zhou, L.; Feng, T.; Xu, S.; Gao, F.; Lam, T.T.; Wang, Q.; Wu, T.; Huang, H.; Zhan, L.; Li, L.; et al. ggmsa: a visual exploration tool for multiple sequence alignment and associated data. *Briefings in Bioinformatics* **2022**, *23*, bbac222. 10.1093/bib/bbac222

 doi:10.20944/preprints202503.0048.v1

128. Charif, D.; Lobry, J.R. *Structural Approaches to Sequence Evolution: Molecules, Networks, Populations*; Bastolla, U., Porto, M., Roman, H.E., Vendruscolo, M., Eds.; Springer Berlin Heidelberg: 2007.
129. Jones, D.T.; Taylor, W.R.; Thornton, J.M. The rapid generation of mutation data matrices from protein sequences. *Comput Appl Biosci* **1992**, *8*, 275-282. 10.1093/bioinformatics/8.3.275